Trends in Renewable Energy
OPEN ACCESS ISSN:2376-2144
Peer-Reviewed Article futureenergysp.com/index.php/tre

Virtual Topologies for Populating Overhead Low-Voltage Broadband over Powerlines Topology Classes by Exploiting Neural Network Topology Generator Methodology (NNTGM) - Part 1: Theory

Athanasios G. Lazaropoulos*

School of Electrical and Computer Engineering / National Technical University of Athens / 9 Iroon Polytechniou Street / Zografou, GR 15780

Received July 23, 2024; Accepted September 1, 2024; Published September 8, 2024

Based on a set of indicative overhead low voltage broadband over power lines (OV LV BPL) topologies of respective OV LV BPL topology classes, Neural Network Topology Generator Methodology (NNTGM) is theoretically proposed in this paper, so that its generated OV LV BPL topologies (NNTGM OV LV BPL topologies) can populate the OV LV BPL topology classes. Given the indicative topology of the OV LV BPL topology class, the NNTGM OV LV BPL topologies can be statistically familiar with the corresponding indicative OV LV BPL topology in terms of the theoretical channel attenuation behavior. Actually, NNTGM is based on the reverse procedure of the Neural Network Identification Methodology for the distribution line and branch Line Length Approximation (NNIM-LLA); say, NNTGM generates theoretical channel attenuation behaviors given the number of branches, the distribution line lengths and the branch line lengths, when appropriate NNTGM default operation settings are assumed. The statistical familiarity between the examined indicative OV LV BPL topology and an NNTGM OV LV BPL topology is examined after the application of appropriate channel attenuation metrics. On the basis of the channel attenuation metrics, class maps are theoretically defined so that the relative positions of indicative OV LV BPL topologies and their respective NNTGM OV LV BPL topologies (NNTGM virtual topologies) can be further studied.

Keywords: Smart Grid; Broadband over Power Lines (BPL) Networks; Power Line Communications (PLC); Distribution and Transmission Power Grids; Neural Networks; Simulation; Modeling

Introduction

Among the communications solutions that can be integrated across the smart grid in order to support its intelligent IP-based communications network of two-way information flows, Broadband over Power Lines (BPL) networks may exploit the available wired power grid infrastructure without investing additional costs in networking cables [1-7].

Deterministic Hybrid Model (DHM), which describes the BPL signal propagation and transmission across the topologies of the overhead low voltage (OV LV) BPL networks while feeding the Topology Identification Methodology (TIM) BPL topology database with the big data of the operation of OV LV BPL topologies, is considered to be

*Corresponding author: AGLazaropoulos@gmail.com

the channel model basis where all the artificial intelligence (AI), machine learning (ML) and neural network (NN) features have been built on [3, 4, 8-16]. As the added AI - ML - NN functionalities are concerned, the neural network identification methodology for the branch number identification (NNIM-BNI) of OV LV BPL topologies has been proposed in [17]. Then, the neural network identification methodology for the distribution line and branch line length approximation (NNIM-LLA) has been proposed for the OV LV BPL topologies in [2] while its performance has been assessed for various usage scenarios in [6, 7]. Actually, NNIM-LLA approximates the distribution line and branch line lengths for a given OV LV BPL topology theoretical channel attenuation behavior thus performing the tomography of the OV LV BPL topology.

In this paper, the Neural Network Topology Generator Methodology (NNTGM) is theoretically proposed and aims at reversing the operation of NNIM-LLA so that virtual topologies can populate existing OV LV BPL topology classes [18-21]. For the NNTGM operation, the available big data of the TIM BPL topology database for the OV LV BPL topologies of [15, 16], the NN architectures / training / methodology of [2, 17] and the conclusions for better approximation performances for the family products of TIM and NNIM of [2, 6, 7, 17] are exploited. The NNTGM output is a collection of NNTGM virtual topologies that present only theoretical channel attenuation behaviors when their topological characteristics are set to be derived from the topological characteristics of the indicative OV LV BPL topology of the examined class that anyway acts as the basis for the topological characteristics of the NNTGM virtual topologies. In accordance with [2, 6, 7, 17], since default operation settings play a critical role in the operation of the family products of TIM and NNIM, they are also going to determine the operation of NNTGM. However, the NNTGM default operation settings, which are going to be analytically reported in this paper, are different from the NNIM-based ones in terms of the preparation parameters of the TIM OV LV BPL topology database since the vicinity to the examined indicative OV LV BPL topology is of interest for NNTGM rather than the representativeness of all the OV LV BPL topologies.

To examine the statistical familiarity of the NNTGM virtual topologies with the respective indicative OV LV BPL topologies, channel attenuation metrics, such as the average theoretical channel attenuation (ACA) and the root mean square delay-spread (RMS-DS), are going to be exploited. With reference to [18-22], new OV LV BPL topology class maps are here defined by the graphical ACA / RMS-DS combination of their respective indicative OV LV BPL topologies. NNTGM virtual topologies that come from an indicative OV LV BPL topology graphically define the NNTGM virtual topology footprint of the indicative OV LV BPL topology. The graphical vicinity of the NNTGM virtual topology footprints to their respective indicative OV LV BPL topologies is examined on the OV LV BPL topology class maps. Then, the impact of the parameters of the NNTGM default operation settings on the relative position and the size of the NNTGM virtual topology footprints are further graphically and numerically assessed in the companion paper [23].

The rest of this paper is organized as follows: Section 2 briefly presents the indicative OV LV BPL topologies of the classes that are going to be used during the benchmark process of these two papers. Also, this Section summarizes the basics of DHM, TIM OV LV BPL topology database and NNIM-LLA as well as NNIM-LLA default operation settings. Section 3 analyzes the operation of the proposed NNTGM. Also, the NNTGM default operation settings and the channel attenuation metrics of ACA and RMS-DS are here reported. Section 4 concludes this paper.

Indicative OV LV BPL Topologies of Topology Classes, DHM, TIM OV LV BPL Topology Database and NNIM-LLA

In this Section, four indicative OV LV BPL topologies that are the representative ones of the four main OV LV BPL topology classes of [18-21, 24] are reported. Then, DHM, which creates the big data pool, and TIM OV LV BPL topology database are briefly discussed. Finally, NNIM-LLA, which is going to be procedurally reversed for the sake of the NNTGM definition, is presented as well as NNIM-LLA default operation settings.

OV LV BPL Topologies and Respective Topology Classes

As already mentioned in [8, 10, 25, 26], OV LV BPL networks are divided into cascaded OV LV BPL topologies of typical lengths of 1000m while a typical OV LV BPL topology is shown in Figure 1. With reference to Figure 1, the typical OV LV BPL topology is bounded by its transmitting and receiving ends. Across the transmission path of the OV LV BPL topology, N branches of open-circuit terminations may occur. The arbitrary k, k=1,…,N branch has length equal to $L_{\mathrm{b}k}$ while it is located at distance $\sum_{i=1}^{k} L_i$ from the transmitting end. In accordance with [2, 10, 17, 25], the topological characteristics and the number of branches for four indicative OV LV BPL topologies – *i.e.*, Line-Of-Sight (LOS), rural, suburban and urban– are listed in Table 1. The aforementioned four indicative OV LV BPL topologies are the representative ones of the respective main OV LV BPL topology classes, which are detailed in [18, 20, 21].

DHM

DHM is a synthetic BPL channel model of three cascaded modules; say, the bottom-up, the top-down and the coupling scheme modules [2, 8-10, 17, 19, 25, 29, 30],. In detail, the bottom-up and top-down modules of DHM address the propagation and transmission issues of the BPL signal across the OV LV BPL topologies, respectively, while the coupling scheme module is responsible for studying the injection / extraction of the BPL signal across the OV LV Multi-conductor Transmission Line (MTL) configurations and the OV LV BPL topologies. The theoretical coupling scheme channel transfer function, which is the output of DHM for given OV LV MTL configuration, OV LV BPL topology and coupling scheme, is stored in the TIM OV LV BPL topology database. Trying different variations on the applied OV LV MTL configurations, OV LV BPL topologies and coupling schemes, TIM OV LV BPL topology database compiles a wealth of case studies thus creating the necessary big data for AI, ML and NNIM-based methodologies to operate.

TIM OV LV BPL Topology Database

In accordance with [2, 17], TIM OV LV BPL topology database has already acted as the big data pool for NNIM-BNI and NNIM-LLA. Depending on the operation scenario, the records of the TIM OV LV BPL topology database for NNIM-BNI and NNIM-LLA may contain the following fields: (i) the ID number p of the OV LV BPL topology when the number of all OV LV BPL topologies in the TIM OV LV BPL topology database is equal to P; (ii) the actual number of branches N of the OV LV BPL topology; (iii) the actual lengths of the distribution lines $\mathbf{L} = [L_1 \quad L_2 \quad \cdots \quad L_{N+1}]$ of each OV LV BPL topology;

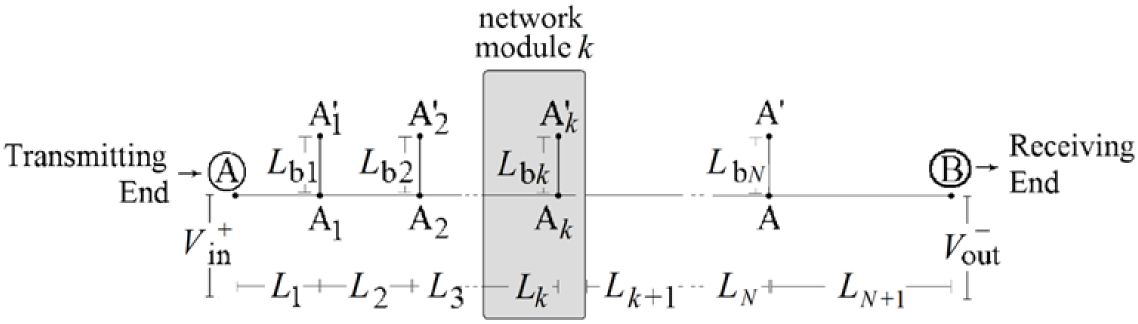

Fig. 1. Typical OV LV BPL topology with *N* branches [17, 27]

Table 1. Indicative OV LV BPL Topologies [10, 17, 18, 20, 21, 25, 28]

OV LV BPL Topology Name	OV LV BPL Topology Class Name	Branch Number (*N*)	Length of Main Lines	Length of Branches
Urban case A (Typical urban case)	Urban	3	L_1=500m, L_2=200m, L_3=100m, L_4=200m	L_{b1}=8m, L_{b2}=13m, L_{b3}=10m
Suburban case	Suburban	2	L_1=500m, L_2=400m, L_3=100m	L_{b1}=50m, L_{b2}=10m
Rural case	Rural	1	L_1=600m, L_2=400m	L_{b1}=300m
LOS case	LOS	0	L_1=1000m	-

(iv) the actual lengths of the branch lines $\mathbf{L_b} = [L_{b1} \quad L_{b2} \quad \cdots \quad L_{bN}]$ of each OV LV BPL topology; and (v) the theoretical coupling scheme channel transfer function values with respect to the frequency. Here, it should be noted that the size of the TIM OV LV BPL topology database, which further affects the performance and the execution times of the family products of NNIM-based methodologies, depends on the default operation settings that are applied and are presented in the following subsection.

NNIM-LLA and NNIM-LLA Default Operation Settings

NNIM-LLA has first been presented in [2] while its performance has been assessed during various operation scenarios in [6, 7]. NNIM-LLA is based on an NN architecture where its fully connected NN of *HL* hidden layers of neurons receives as input the amplitude of the coupling scheme channel transfer functions of the OV LV BPL topologies of the TIM OV LV BPL topology database in dB and gives as output the NNIM-LLA approximation for the lengths of the examined indicative OV LV BPL topology (*i.e.*, the NNIM-LLA approximation lengths of the distribution and branch lines are $\mathbf{L}_{\text{NNIM-LLA}} = [L_{1,\text{NNIM-LLA}} \quad L_{2,\text{NNIM-LLA}} \quad \cdots \quad L_{N+1,\text{NNIM-LLA}}]$ and $\mathbf{L}_{\text{b,NNIM-LLA}} = [L_{\text{b1,NNIM-LLA}} \quad L_{\text{b2,NNIM-LLA}} \quad \cdots \quad L_{\text{b}N\text{,NNIM-LLA}}]$, respectively). Actually, NNIM-LLA approximates the distribution line and branch line lengths of the examined OV LV BPL topology when its OV LV BPL topology theoretical channel attenuation behavior is separately fed to NNIM-LLA. The core of NNIM-LLA is its MATLAB NN training program, which is detailed in [31, 32], that jointly processes the big data of the TIM OV LV BPL topology database with the OV LV BPL topology theoretical channel attenuation. The MATLAB NN training program is divided into three phases; say, training, validation and testing phases, while these three phases segment the big data of the TIM OV LV BPL topology database in accordance with the respective participation percentages. In accordance with [2, 6, 7], the critical factor for the high performance and accuracy of NNIM-LLA is the selection of appropriate NNIM-LLA default operation settings.

According to [2, 6, 7, 17], the adoption of elaborate NNIM-LLA default operation settings, which may support higher accuracies for the TIM OV LV BPL topology database, can significantly improve the performance of NNIM-LLA. The NNIM-LLA operation settings that can be configured for the included OV LV BPL topologies in the TIM OV LV BPL topology database and for the operation of the MATLAB NN training program are: (i) the number of branches; (ii) the length spacings for the branch distance and the branch length; (iii) the branch line length range; (iv) the total distribution line length; (v) the coupling scheme; (vi) the frequency range; (vii) the flat-fading subchannel frequency spacing; and (viii) the default participation percentages of the three phases. However, a trade-off between the accuracy of the applied default operation settings and the total execution time of NNIM-LLA has been revealed in [6].

NNTGM is going to be the procedural reversal of NNIM-LLA while NNTGM default operation settings are going to exploit the NNIM-LLA ones and the good practices learned from their study. NNTGM is first presented in the coming Section.

NNTGM: Definition, Default Operation Settings, Channel Attenuation Metrics and Class Maps

In this Section, NNTGM is proposed based on the NNIM-based family products; say, NNIM-BNI and NNIM-LLA. Apart from its definition, NNTGM default operation settings are reported while their parameters that are going to be configured for the included OV LV BPL topologies in the TIM OV LV BPL topology database are discussed. Finally, the channel attenuation metrics of ACA and RMS-DS are mathematically defined so that they can be applied to the indicative OV LV BPL topologies and their respective NNTGM virtual OV LV BPL topologies for the preparation of the OV LV BPL topology class maps.

NNTGM Definition

With reference to Figure 2 of [2] and [17], NNTGM is going to implement the inverted NN architecture that has been applied in NNIM-BNI and NNIM-LLA. The structure of the NNTGM fully connected NN is assumed to have *HL* hidden layers of neurons. The input of the NN is *P* column vectors where *P* is the total number of the used OV LV BPL topologies that come from the records of the TIM OV LV BPL topology database while the *p*, *p*=1,…,*P* column vector consists of the actual lengths of the distribution and branch lines of the arbitrary *p* OV LV BPL topology of the TIM OV LV BPL topology database, namely:

$$\mathbf{L}_{\mathrm{TIM},p,hl=0}^{\mathrm{OVLV,C}}\{\cdot\} = [\mathbf{L}_p \quad \mathbf{L}_{\mathrm{b},p}]^{\mathrm{T}} = [L_{1,p} \quad L_{2,p} \quad \cdots \quad L_{N+1,p} \quad L_{\mathrm{b1},p} \quad L_{\mathrm{b2},p} \quad \cdots \quad L_{\mathrm{b}N,p}]^{\mathrm{T}} \quad (1)$$

where $[\cdot]^{\mathrm{T}}$ denotes the transpose of the matrix and each column vector consists of $\underbrace{N+1}_{\text{number of main lines}} + \underbrace{N}_{\text{number of branches}} = 2N+1$ lines. After the input layer, *HL* hidden layers occur. The output of the fully connected NN is a $Q \times 1$ channel attenuation difference column vector that is given by

$$\Delta\mathbf{H}^{\mathrm{OVLV,C}}\{\cdot\} = [\left|H_{\mathrm{NNTGM}}^{\mathrm{OVLV,C}}(f_1)\right|_{\mathrm{dB}} - \left|H_{\mathrm{LOS}}^{\mathrm{OVLV,C}}(f_1)\right|_{\mathrm{dB}} \cdots$$
$$\cdots \left|H_{\mathrm{NNTGM}}^{\mathrm{OVLV,C}}(f_q)\right|_{\mathrm{dB}} - \left|H_{\mathrm{LOS}}^{\mathrm{OVLV,C}}(f_q)\right|_{\mathrm{dB}} \cdots \left|H_{\mathrm{NNTGM}}^{\mathrm{OVLV,C}}(f_Q)\right|_{\mathrm{dB}} - \left|H_{\mathrm{LOS}}^{\mathrm{OVLV,C}}(f_Q)\right|_{\mathrm{dB}}]^{\mathrm{T}} \quad (2)$$

where $\left|H_{\mathrm{NNTGM}}^{\mathrm{OVLV,C}}\{\cdot\}\right|_{\mathrm{dB}}$ is the amplitude of the coupling scheme channel transfer function of the NNTGM generated OV LV BPL topology in dB, $\left|H_{\mathrm{LOS}}^{\mathrm{OVLV,C}}\{\cdot\}\right|_{\mathrm{dB}}$ is the amplitude of the coupling scheme channel transfer function of LOS case of Table 1 in dB, $[\cdot]^{\mathrm{C}}$ denotes the applied coupling scheme and $f_q, q = 1, \dots, Q$ are the operating frequencies when the examined frequency range is divided into Q flat-fading subchannels. With reference to eq. (2), the output of the NNTGM is the $Q \times 1$ NNTGM generated channel attenuation column vector that is given by

$$\mathbf{H}_{\mathrm{NNTGM}}^{\mathrm{OVLV,C}}\{\cdot\} = \Delta\mathbf{H}^{\mathrm{OVLV,C}}\{\cdot\} +$$
$$+[\left|H_{\mathrm{LOS}}^{\mathrm{OVLV,C}}(f_1)\right|_{\mathrm{dB}} \cdots \left|H_{\mathrm{LOS}}^{\mathrm{OVLV,C}}(f_q)\right|_{\mathrm{dB}} \cdots \left|H_{\mathrm{LOS}}^{\mathrm{OVLV,C}}(f_Q)\right|_{\mathrm{dB}}]^{\mathrm{T}} \quad (3)$$

As the operation of the NNTGM fully connected NN is concerned, NNTGM is based on the MATLAB NN training program of [31, 32] where the inner big data handling of the TIM OV LV BPL topology database is divided into training, validation and testing phases with respective participation percentages. In fact, the MATLAB NN training program randomly splits the supplied big data from the TIM OV LV BPL topology database into 3 portions in accordance with the aforementioned participation percentages of the three phases. In addition, training is achieved using the Levenberg-Marquardt algorithm while RMS-DS is the applied criterion for deciding the best NN approximation of the MATLAB NN training program.

To generate NNTGM virtual topologies for given indicative OV LV BPL topology, the option of testing additional external data that may be offered to the MATLAB NN training program is exploited while appropriately defining the insertions of the TIM OV LV BPL topology database. In contrast with the preparation of the TIM OV LV BPL topology database for NNIM-BNI and NNIM-LLA, TIM OV LV BPL topology database for NNTGM should contain only OV LV BPL topologies with the lengths of the distribution and branch lines that remain close to the respective values of the examined indicative OV LV BPL topology since NNTGM virtual topologies are expected to present only theoretical channel attenuation behaviors when their topological characteristics are assumed to be the same with the topological characteristics of the indicative OV LV BPL topology of the examined class. Hence, with reference to eq. (2), the actual lengths of the distribution and branch lines of the arbitrary p OV LV BPL topology during the preparation of the TIM OV LV BPL topology database for NNTGM are bounded as follows:

$$L_{i,p} - L_{\mathrm{s}} \cdot t_{\mathrm{s}} \leq L_{i,p} \leq L_{i,p} + L_{\mathrm{s}} \cdot t_{\mathrm{s}}, \;\; L_{i,p} - L_{\mathrm{s}} \cdot t_{\mathrm{s}} \geq 0, \;\; i=1,\dots,N \quad (4)$$

$$L_{i,p} \in \{L_{i,p} \pm L_s \cdot t | t \in \{0, \cdots, t_s\}, t \in \mathbb{Z}^{0+} \}, \;\; i=1,\dots,N \quad (5)$$

$$L_{N+1,p} = 1{,}000m - \sum_{i=1}^{N} L_{i,p} \quad (6)$$

$$L_{bi,p} - L_{\mathrm{bs}} \cdot t_{\mathrm{bs}} \leq L_{bi,p} \leq L_{bi,p} + L_{\mathrm{bs}} \cdot t_{\mathrm{bs}}, \;\; L_{bi,p} - L_{\mathrm{bs}} \cdot t_{\mathrm{bs}} \geq 0, \;\; i=1,\dots,N \quad (7)$$

$$L_{bi,p} \in \{L_{bi,p} \pm L_{bs} \cdot t | t \in \{0, \cdots, t_{bs}\}, t \in \mathbb{Z}^{0+} \}, \;\; i=1,\dots,N \quad (8)$$

where L_{s} and L_{bs} are the length of the distribution and branch line segments, respectively, and t_{s} and t_{bs} are the number of the distribution and branch line segments that are going to be used during the preparation of the TIM OV LV BPL topology database for NNTGM operation, respectively. From eqs. (4)-(8), given $L_{\mathrm{s}} \cdot t_{\mathrm{s}}$ and $L_{\mathrm{bs}} \cdot t_{\mathrm{bs}}$ remain relatively small, the following observations concerning the preparation of the TIM OV LV BPL topology database are given:

- The total number of the OV LV BPL topologies that are going to be added in the TIM OV LV BPL topology database is equal to:

$$P = \underbrace{(2 \cdot t_{\mathrm{s}} + 1)^N}_{eqs.(4)-(6)} \cdot \underbrace{(2 \cdot t_{\mathrm{bs}} + 1)^N}_{eqs.(7),(8)} \tag{9}$$

  when the examined indicative OV LV BPL topology is included into the TIM OV LV BPL topology database during the NNTGM operation. Conversely, when the examined indicative OV LV BPL topology is omitted from the TIM OV LV BPL topology database during the NNTGM operation, the total number of the OV LV BPL topologies from the TIM OV LV BPL topology database becomes equal to:

$$P = \underbrace{(2 \cdot t_{\mathrm{s}})^N}_{eqs.(4)-(6)} \cdot \underbrace{(2 \cdot t_{\mathrm{bs}})^N}_{eqs.(7),(8)} \tag{10}$$

  It is evident that the inclusion or not of the examined indicative OV LV BPL topology in the TIM OV LV BPL topology database may affect the degree of variation of the amplitude of the coupling scheme channel transfer function of the NNTGM generated OV LV BPL topologies in dB with respect to the amplitude of the coupling scheme channel transfer function of LOS case. The impact assessment of the inclusion or not of the examined indicative OV LV BPL topology in the TIM OV LV BPL topology database on the NNTGM performance is going to be numerically evaluated in the companion paper of [23].
- Apart from the total number of the OV LV BPL topologies that is going to be contained in the TIM OV LV BPL topology database for the NNTGM operation purposes as given in eqs. (9) and (10), the length and the number of distribution and branch line segments may further affect the degree of variation of the amplitude of the coupling scheme channel transfer function of the NNTGM generated OV LV BPL topologies in dB with respect to the amplitude of the coupling scheme channel transfer function of LOS case. Higher lengths and numbers of distribution and branch line segments entail higher variations of the amplitude of the coupling scheme channel transfer function of the NNTGM virtual OV LV BPL topologies due to the variety of the channel attenuation behaviors of the OV LV BPL topologies that are contained in the TIM OV LV BPL topology database. The assessment of the NNTGM virtual OV LV BPL topologies can be done by applying channel attenuation metrics such as the ACA and RMS-DS. Anyway, the lengths and numbers of distribution and branch line segments remain an essential part of the NNTGM default operation settings as theoretically shown in eqs. (4)-(8).
- The graphical vicinity of the NNTGM virtual topologies with their respective indicative OV LV BPL topologies is examined on the OV LV BPL topology class maps. The OV LV BPL topology class maps of this pair of papers are going to be plotted with reference to ACA and RMS-DS while the indicative OV LV BPL topologies of Table 1 will define their respective class map footprint center. Given the TIM OV LV BPL topology database and the examined indicative OV LV BPL topology, the respective NNTGM virtual topologies may define an NNTGM virtual topology footprint while its extent and its relative position inside the class of the corresponding indicative OV LV BPL topology depend on several factors with reference to eqs. (4)-(10), such as: (i) The inclusion or not of the examined indicative OV LV BPL topology in the TIM OV LV BPL topology

database during the NNTGM operation; (ii) the length of the distribution / branch line segments; and (iii) the number of the distribution / branch line segments. Note that 100 NNTGM virtual topologies are assumed to be generated per each OV LV BPL topology class and thus per indicative OV LV BPL topology excluding the LOS class. The correlation among the length and the number of distribution and branch line segments and the extent and relative position of the NNTGM virtual topology footprints are going to be investigated in the companion paper [23]. In the following subsection, the parameters of the NNTGM default operation settings that are going to be configured for the included OV LV BPL topologies of the TIM OV LV BPL topology database, which have already been defined in this subsection, are discussed.

NNTGM Default Operation Settings

In contrast with the default operation settings of NNIM-BNI and NNIM-LLA, the NNTGM default operation settings are strictly based on the database representativeness principle of [2] rather than the richness and the diversity of the applied big data, namely:

- For given examined indicative OV LV BPL topology, its number of the branches and its actual lengths of the distribution and branch lines are assumed to be known thus the OV LV BPL topologies that are going to be included in the TIM OV LV BPL topology database are defined by eqs. (4)-(8) in each case. For given examined indicative OV LV BPL topology, the total number of the OV LV BPL topologies that are added in the TIM OV LV BPL topology database is given in eq. (9) with the inclusion of the indicative OV LV BPL topology in the TIM OV LV BPL topology database that is the default option of the parameter. If the indicative OV LV BPL topology is excluded from the TIM OV LV BPL topology database, which is the variant option of the parameter, the total number of the OV LV BPL topologies that are added in the TIM OV LV BPL topology database is given from eq. (10) while t of eq. (5) and eq. (8) deals with only the positive integers. As the default operation setting values are concerned in this pair of papers, the length of the distribution and branch line segments are assumed to be equal to 1m and 1m, respectively, while the number of the distribution and branch line segments are assumed to be equal to 1 and 1, respectively. It is clear that the aforementioned NNTGM default operation setting parameter selection focuses on generating NNTGM virtual topology footprints that derive from the examined indicative OV LV BPL topology in each scenario while higher values of the aforementioned parameters are expected to relax the relative position and the extent of the NNTGM virtual topology footprints.
- The total distribution line length is assumed to be equal to 1,000 m in all the OV LV BPL topologies of the TIM OV LV BPL topology database. Also, the terminations of all the OV LV BPL topologies of the TIM OV LV BPL topology are assumed to be open-circuit ones in a similar way to the indicative OV LV BPL topologies of Table 1. With reference to [11, 33], the applied coupling scheme of interest in this pair of papers is the WtG[1] one.
- As the operating frequencies of interest are concerned in this pair of papers, the frequency range is assumed to be equal to 1-30 MHz while the flat-fading subchannel frequency spacing is equal to 1 MHz. Hence, the number of flat-fading subchannels is equal to 29. With reference to eq. (2), the amplitudes of the coupling scheme channel transfer functions are stored in dB in the TIM OV LV

BPL topology database for its OV LV BPL topologies with respect to the frequency.

- As the NNTGM is based on the MATLAB NN training program of [31, 32], the default participation percentages of the three phases of NNIM-BNI and NNIM-LLA of [2, 17, 31, 32] are also assumed in this pair of papers; say, training, validation and testing phases during the operation of NNTGM are assumed to be equal to 70%, 15% and 15%, respectively.

Apart from the default operation settings, to assess the performance of NNTGM, the channel attenuation metrics of ACA and RMS-DS are mathematically defined in the following subsection. Also, the definition of the aforementioned channel attenuation metrics remains a crucial task for the design of the OV LV BPL topology class maps as well as the impact evaluation of the operation settings of this subsection on the NNTGM virtual topology footprints.

NNTGM Channel Attenuation Metrics and NNTGM Topology Class Maps

With reference to eq. (3), the output of the NNTGM is the $Q \times 1$ NNTGM generated channel attenuation column vector $\mathbf{H}_{\mathrm{NNTGM}}^{\mathrm{OVLV,C}}\{\cdot\}$ for each of the generated OV LV BPL topologies. Based on the NNTGM generated channel attenuation column vector, the NNTGM channel attenuation metrics of ACA and RMS-DS can be mathematically defined, as follows [22]:

- *ACA*: As the BPL channel is frequency selective and f_q, $q = 1, \ldots, Q$ are the operating frequencies when the examined frequency range is divided into Q flat-fading subchannels, ACA can be calculated for each NNTGM virtual topology by averaging over the flat-fading subchannels:

$$ACA_{\mathrm{NNTGM}}^{\mathrm{OVLV,C}} = \frac{1}{Q} \cdot \sum_{q=1}^{Q} \left| H_{\mathrm{NNTGM}}^{\mathrm{OVLV,C}}(f_q) \right|_{\mathrm{dB}} \tag{11}$$

In fact, ACA depends on the multipath nature of the examined OV LV BPL topologies. In accordance with [22], when the number of branches is small and their electrical length is large, like in the rural and suburban cases of Table 1, shallow spectral notches are observed across the theoretical channel attenuation while low values of ACA are expected. Conversely, when the number of branches is large and the electrical length is small, like in the urban case A of Table 1, deep spectral notches are observed across the theoretical channel attenuation while high values of ACA are expected. In accordance with [8, 9, 29, 30], note that LOS case of Table 1 is characterized by the lowest value of ACA among all the OV LV BPL topologies (*i.e.*, either real or NNTGM virtual ones) since no spectral notches are observed. Therefore, NNTGM virtual topologies, which are generated by the respective indicative OV LV BPL topologies of Table 1, are expected to present similar theoretical channel attenuation behaviors and ACA with the ones of the respective indicative OV LV BPL topologies depending on the applied NNGTM operation settings.

- *RMS-DS*: Another channel attenuation metric that assesses the multipath richness of a BPL channel is RMS-DS. With reference to eq. (11), RMS-DS can be calculated for each NNTGM virtual topology as follows:

$$RMS-DS_{\mathrm{NNTGM}}^{\mathrm{OVLV,C}} = \sqrt{\frac{1}{Q} \cdot \sum_{q=1}^{Q} \left[\left| H_{\mathrm{NNTGM}}^{\mathrm{OVLV,C}}(f_q) \right|_{\mathrm{dB}} - ACA_{\mathrm{NNTGM}}^{\mathrm{OVLV,C}} \right]^2} \tag{12}$$

In fact, the RMS-DS measures the average channel attenuation distance from ACA. It is expected that OV LV BPL topologies with rare and shallow spectral notches across their theoretical channel attenuation present low values of RMS-DS whereas OV LV BPL topologies with frequent and deep spectral notches across their theoretical channel attenuation present high values of RMS-DS. Similarly to ACA, NNTGM virtual topologies, which are generated by the respective indicative OV LV BPL topologies of Table 1, are expected to present similar RMS-DS with the one of the respective indicative OV LV BPL topologies depending on the applied NNGTM operation settings.

From eqs. (11) and (12), it is obvious that each OV LV BPL topology can be characterized by a pair of values (ACA, RMS-DS) regardless of being either a real topology or a NNTGM virtual one. Also, the NNTGM virtual topologies are expected to have pairs of values that remain relatively close to the pair of values of their respective indicative OV LV BPL topology of Table 1 thus populating the class of the respective indicative OV LV BPL topology.

Similarly to the class maps of [18, 21, 34-36], new class maps can be plotted where their two axes correspond to the ACA and RMS-DS while each indicative OV LV BPL topology of Table 1 with its NNTGM virtual topologies can define its footprints on the class maps. Since NNTGM virtual topologies are expected to graphically approach their respective indicative OV LV BPL topology, the shape of the footprints of the indicative OV LV BPL topology classes concerning their relative positions and the sizes, depends on the applied NNTGM operation settings.

On the basis of the NNTGM default operation settings of Section 3.2, the impact of the following parameters, which have been identified in this paper, on the relative position and the size of the NNTGM virtual topology footprints is going to be assessed in the companion paper [23]: (i) The inclusion or not of the examined indicative OV LV BPL topology in the TIM OV LV BPL topology database during the NNTGM operation; (ii) the length of the distribution / branch line segments; and (iii) the number of the distribution / branch line segments.

Conclusions

In this first paper, the required theory for populating OV LV BPL topology classes by applying NNTGM has been proposed. First, it has been introduced NNTGM as the new member of the family products of NNIM-based methodologies; say, NNIM-BNI and NNIM-LLA. In fact, it has been shown that NNTGM is based on the reverse procedure of the NNIM-LLA since NNTGM can generate theoretical channel attenuation behaviors given the topological characteristics of an indicative OV LV BPL topology, when appropriate NNTGM operation settings are assumed. Prior to the detailed presentation of NNTGM in this paper, the indicative OV LV BPL topologies of topology classes had been reported while the TIM OV LV BPL topology database and NNIM-LLA, which are critical components for the operation of NNTGM, had been synopsized. Then, the definition of NNTGM has been given focusing on its NN behavior and its mathematical outputs. Apart from the NNTGM default operation settings, the parameters that affect the NNTGM performance and require additional study have been recognized, namely: (i) The inclusion or not of the examined indicative OV LV BPL topology in the TIM OV LV BPL topology database during the NNTGM operation; (ii) the length of the distribution / branch line segments; and (iii) the number of the distribution / branch line segments. Actually, the aforementioned parameters are numerically evaluated in the companion paper of [23] for the OV LV BPL topology classes.

CONFLICTS OF INTEREST

The author declares that there is no conflict of interests regarding the publication of this paper.

References

[1] Lazaropoulos, A. G., & Leligou, H. C. (2022). Fiber optics and broadband over power lines in smart grid: a communications system architecture for overhead high-voltage, medium-voltage and low-voltage power grids. *Progress in Electromagnetics Research B*, *95*, 185-205. doi:http://dx.doi.org/10.2528/PIERB22062502

[2] Lazaropoulos, A. G., & Leligou, H. C. (2023). Artificial Intelligence, Machine Learning and Neural Networks for Tomography in Smart Grid – Performance Comparison between Topology Identification Methodology and Neural Network Identification Methodology for the Distribution Line and Branch Line Length Approximation of Overhead Low-Voltage Broadband over Power Lines Network Topologies. *Trends in Renewable Energy, 9*(1), 34-77. doi:http://dx.doi.org/10.17737/tre.2023.9.1.00149

[3] Amirshahi, P., & Kavehrad, M. (2006). High-frequency characteristics of overhead multiconductor power lines for broadband communications. *IEEE Journal on Selected Areas in Communications*, *24*(7), 1292-1303. doi:https://doi.org/10.1109/JSAC.2006.874399

[4] Sartenaer, T., & Delogne, P. (2006). Deterministic modeling of the (shielded) outdoor power line channel based on the multiconductor transmission line equations. *IEEE Journal on Selected areas in Communications*, *24*(7), 1277-1291. doi:https://doi.org/10.1109/JSAC.2006.874423

[5] Marcuzzi, F., & Tonello, A. M. (2023). Topology-based machine learning: Predicting power line communication quality in smart grids. *IEEE Access*, *11*, 24851-24862. doi:https://doi.org/10.1109/ACCESS.2023.3245361

[6] Lazaropoulos, A. G., & Leligou, H. C. (2024). Big Data and Neural Networks in Smart Grid - Part 1: The Impact of Piecewise Monotonic Data Approximation Methods on the Performance of Neural Network Identification Methodology for the Distribution Line and Branch Line Length Approximation of Overhead Low-Voltage Broadband over Powerlines Networks. *Trends in Renewable Energy, 10*, 30-66. doi:https://doi.org/10.17737/tre.2024.10.1.00164

[7] Lazaropoulos, A. G., & Leligou, H. C. (2024). Big Data and Neural Networks in Smart Grid - Part 2: The Impact of Piecewise Monotonic Data Approximation Methods on the Performance of Neural Network Identification Methodology for the Distribution Line and Branch Line Length Approximation of Overhead Low-Voltage Broadband over Powerlines Networks. *Trends in Renewable Energy, 10*, 67-97. doi:https://doi.org/10.17737/tre.2024.10.1.00165

[8] Lazaropoulos, A. G., & Cottis, P. G. (2009). Transmission characteristics of overhead medium voltage power line communication channels. *IEEE Transactions on Power Delivery*, *24*(3), 1164-1173. doi:https://doi.org/10.1109/TPWRD.2008.2008467

[9] Lazaropoulos, A. G., & Cottis, P. G. (2010). Capacity of overhead medium voltage power line communication channels. *IEEE Transactions on Power Delivery*, *25*(2), 723-733. doi:https://doi.org/10.1109/TPWRD.2009.2034907

[10] Lazaropoulos, A. G. (2012). Towards Modal Integration of Overhead and Underground Low-Voltage and Medium-Voltage Power Line Communication Channels in the Smart Grid Landscape: Model Expansion, Broadband Signal Transmission Characteristics, and Statistical Performance Metrics (Invited Paper). *International Scholarly Research Notices, 2012*(1), 121628. doi:https://doi.org/10.5402/2012/121628

[11] Lazaropoulos, A. G. (2016). New coupling schemes for distribution broadband over power lines (BPL) networks. *Progress in Electromagnetics Research B*, *71*, 39-54. doi:http://dx.doi.org/10.2528/PIERB16081503

[12] Amirshahi-Shirazi, P. (2006). *Broadband access and home networking through powerline networks*. The Pennsylvania State University. Ph.D. dissertation.

[13] Sartenaer, T. (2004). *Multiuser communications over frequency selective wired channels and applications to the powerline access network* (Doctoral dissertation, Catholic University of Louvain, Louvain-la-Neuve, Belgium).

[14] Sartenaer, T., & Delogne, P. (2001). Powerline cables modelling for broadband communications. In *Proceedings of the IEEE International Conference on Power Line Communications and Its Applications*, Malmö, Sweden, pp. 331-337.

[15] Lazaropoulos, A. G. (2017). Improvement of Power Systems Stability by Applying Topology Identification Methodology (TIM) and Fault and Instability Identification Methodology (FIIM) Study of the Overhead Medium-Voltage Broadband over Power Lines (OV MV BPL) Networks Case. *Trends in Renewable Energy, 3*(2), 102-128. doi:http://dx.doi.org/10.17737/tre.2017.3.2.0034

[16] Lazaropoulos, A. G. (2016). Measurement Differences, Faults and Instabilities in Intelligent Energy Systems - Part 1: Identification of Overhead High-Voltage Broadband over Power Lines Network Topologies by Applying Topology Identification Methodology (TIM). *Trends in Renewable Energy, 2*, 85-112. doi: http://dx.doi.org/10.17737/tre.2016.2.3.0026

[17] Lazaropoulos, A. G. (2021). Information Technology, Artificial Intelligence and Machine Learning in Smart Grid – Performance Comparison between Topology Identification Methodology and Neural Network Identification Methodology for the Branch Number Approximation of Overhead Low-Voltage Broadband over Power Lines Network Topologies. *Trends in Renewable Energy, 7*, 87-113. doi:http://dx.doi.org/10.17737/tre.2021.7.1.00133

[18] Lazaropoulos, A. G. (2020). Business Analytics and IT in Smart Grid - Part 1: The Impact of Measurement Differences on the iSHM Class Map Footprints of Overhead Low-Voltage Broadband over Power Lines Topologies. *Trends in Renewable Energy, 6*(2), 156-186. doi:http://dx.doi.org/10.17737/tre.2020.6.2.00117

[19] Lazaropoulos, A. G. (2020). Statistical Channel Modeling of Overhead Low Voltage Broadband over Power Lines (OV LV BPL) Networks - Part 1: The

Theory of Class Map Footprints of Real OV LV BPL Topologies, Branch Line Faults and Hook-Style Energy Thefts. *Trends in Renewable Energy, 6*(1), 61-87. doi:http://dx.doi.org/10.17737/tre.2020.6.1.00112

[20] Lazaropoulos, A. G. (2020). Business Analytics and IT in Smart Grid - Part 2: The Qualitative Mitigation Impact of Piecewise Monotonic Data Approximations on the iSHM Class Map Footprints of Overhead Low-Voltage Broadband over Power Lines Topologies Contaminated by Measurement Differences. *Trends in Renewable Energy, 6*(2), 187-213. doi:http://dx.doi.org/10.17737/tre.2020.6.2.00118

[21] Lazaropoulos, A. G. (2020). Business Analytics and IT in Smart Grid - Part 3: New Application Aspect and the Quantitative Mitigation Analysis of Piecewise Monotonic Data Approximations on the iSHM Class Map Footprints of Overhead Low-Voltage Broadband over Power Lines Topologies Contaminated by Measurement Differences. *Trends in Renewable Energy, 6*(2), 214-233. doi:http://dx.doi.org/10.17737/tre.2020.6.2.00119

[22] Lazaropoulos, A. G. (2012). Broadband Transmission and Statistical Performance Properties of Overhead High-Voltage Transmission Networks. *Journal of Computer Networks and Communications, 2012*(1), 875632. doi:https://doi.org/10.1155/2012/875632

[23] Lazaropoulos, A. (2024). Virtual Topologies for Populating Overhead Low-Voltage Broadband over Powerlines Topology Classes by Exploiting Neural Network Topology Generator Methodology (NNTGM) - Part 2: Numerical Results. *Trends in Renewable Energy, 10*(3), 315-334. doi:http://dx.doi.org/10.17737/tre.2024.10.3.00182

[24] Lazaropoulos, A. (2020). Statistical Channel Modeling of Overhead Low Voltage Broadband over Power Lines (OV LV BPL) Networks - Part 2: The Numerical Results of Class Map Footprints of Real OV LV BPL Topologies, Branch Line Faults and Hook Style Energy Thefts. *Trends in Renewable Energy, 6*(1), 88-109. doi:http://dx.doi.org/10.17737/tre.2020.6.1.00113

[25] Lazaropoulos, A. G. (2013). Review and Progress towards the Capacity Boost of Overhead and Underground Medium-Voltage and Low-Voltage Broadband over Power Lines Networks: Cooperative Communications through Two- and Three-Hop Repeater Systems. *International Scholarly Research Notices, 2013*(1), 472190. doi:https://doi.org/10.1155/2013/472190

[26] Meng, H., Chen, S., Guan, Y. L., Law, C. L., So, P. L., Gunawan, E., & Lie, T. T. (2004). Modeling of transfer characteristics for the broadband power line communication channel. *IEEE Transactions on Power delivery*, *19*(3), 1057-1064. doi:https://doi.org/10.1109/TPWRD.2004.824430

[27] Lazaropoulos, A. G. (2019). Statistical broadband over power lines channel modeling-Part 1: The theory of the statistical hybrid model. *Progress in Electromagnetics Research C*, *92*, 1-16. doi:http://dx.doi.org/10.2528/PIERC19012902

[28] Qu, B., Wang, H., Chen, Z., Zheng, Z., Han, Z., & Zhang, L. (2021). A Channel Selection Algorithm of Power Line Communication Network Base on Double-layer Cascade Artificial Neural Network. *Journal of Physics: Conference Series*, *2031*(1), 012041. doi:http://dx.doi.org/10.1088/1742-6596/2031/1/012041

[29] Lazaropoulos, A. G., & Cottis, P. G. (2010). Broadband transmission via underground medium-voltage power lines-Part I: transmission characteristics.

IEEE Transactions on Power Delivery, *25*(4), 2414-2424. doi:https://doi.org/10.1109/TPWRD.2010.2048929

[30] Lazaropoulos, A. G., & Cottis, P. G. (2010). Broadband transmission via underground medium-voltage power lines-Part II: capacity. *IEEE Transactions on Power Delivery*, 25(4), 2425-2434. doi:https://doi.org/10.1109/TPWRD.2010.2052113

[31] Okoh, D. (2016). *Computer neural networks on MATLAB*. CreateSpace Independent Publishing Platform.

[32] Okoh, D. (2020). *Neural Network Training Code*. Available at: https://www.mathworks.com/matlabcentral/fileexchange/59362-neural-network-training-code (Accessed: 22 April 2020).

[33] Lazaropoulos, A. G. (2018). Broadband Performance Metrics and Regression Approximations of the New Coupling Schemes for Distribution Broadband over Power Lines (BPL) Networks. *Trends in Renewable Energy, 4*(1), 43-73. doi:http://dx.doi.org/10.17737/tre.2018.4.1.0059

[34] Lazaropoulos, A. G. (2019). Virtual Indicative Broadband over Power Lines Topologies for Respective Subclasses by Adjusting Channel Attenuation Statistical Distribution Parameters of Statistical Hybrid Models (Class Maps) – Part 1: Theory. *Trends in Renewable Energy*, *5*(3), 237-257. doi:http://dx.doi.org/10.17737/tre.2019.5.3.0099

[35] Lazaropoulos, A. G. (2019). Virtual Indicative Broadband over Power Lines Topologies for Respective Subclasses by Adjusting Channel Attenuation Statistical Distribution Parameters of Statistical Hybrid Models (Class Maps) – Part 2: Numerical Results for the Overhead and Underground Medium-Voltage Power Grids. *Trends in Renewable Energy*, *5*(3), 258-281. doi:http://dx.doi.org/10.17737/tre.2019.5.3.00100

[36] Lazaropoulos, A. G. (2019). Virtual Indicative Broadband over Power Lines Topologies for Respective Subclasses by Adjusting Channel Attenuation Statistical Distribution Parameters of Statistical Hybrid Models (Class Maps) – Part 3: The Case of Overhead Transmission Power Grids. *Trends in Renewable Energy*, 5(3), 282-306. doi:http://dx.doi.org/10.17737/tre.2019.5.3.00101